Root-Cause Analysis of Interfered Current Transformer Due to Pulsed Currents

Leonardo Bolzonella s2367963
University Of Twente
Enschede, The Netherlands
l.bolzonella@student.utwente.nl

***Abstract*—With the widespread use in recent years of non-linear loads that draw pulsed currents with large d*i*/d*t*, crest factor and amplitude, an increase in EMI was detected on meters, resulting in power metering deviations. In particular, the type of sensor determines the overall deviations: Rogowski coil sensing resulted in errors up to 400%, Hall sensors negative deviations up to -10%, and current transformer in deviations between -10% and 8%. Generally, this resulted in large over-billing of costumers by the hands of utility companies. In this paper the source and implications of the metering interference are analysed for pulsed currents using current transformer sensing. It was noted that pulsed current metering using current transformer incurs in two issues: firstly, the large DC components of the pulse does not induce a secondary current in the transformer, and secondly, the magnetization behavior of the core results in an exponential response. Additionally, the primary pulse width determined the asymmetric behaviour in secondary response, and the small value of load cause a large time constant, and therefore large settling times. Together, these issues result in erroneous current waveform measurements. Finally, the correlation between firing angle and error magnitude and sign is analysed, correlating positive deviations for firing angles above 90 degrees, negative below 90 degrees, and minimal absolute error around 90 degrees. Overall, this research shows the unsuitability of current transformer metering for pulsed currents, as well as the need of additional testing, even for energy meters compliant with current EMI test standards, which will help ensure fair and precise billing of customers by the utilities.**

I. Introduction

Static energy meters are devices installed in households to measure electric power consumption on behalf of utility companies, in order to accurately and fairly bill the costumers. On the other hand, the widespread use of non-linear loads (such as dimming LED lights or remotes), in the recent years resulted in an increase in electromagnetic interference (EMI) in static meters, causing under or over-billing of costumers by the utilities. Previous research has shown the presence of EMI on static meters causing measuring errors up to 2000%, even on recent meters that comply with EMI test standard IEC 61000-4-19 [1]. These large deviations usually result in large over-billing of costumers. Even after costumer complaints, utilities rejected those claims, stating that the old metering devices were underestimating power consumption due to mechanical wear on the sensors [2]. Particularly, non-linear loads that draw pulsed currents with high d*i*/d*t*, large amplitude and crest factor are known to create large deviation issues. In [2] the metering error is identified for three types of current metering sensors: Rogowski coil, current transformer (CT) and Hall sensor. It was noted that the type of current sensor included within the smart meter determined the overall deviation. Notably, a positive deviation between 200% and 500% was recorded for Rogowski coil, while a negative deviation between -30% and -40% for Hall sensors. Finally, deviations between -8% and +10% were measured for current transformer sensors. A root cause analysis was performed, concluding that the value of the firing angle (FA) of the pulsed currents was correlated with the magnitude of the deviation. In [3], another case of erroneous power metering was reported by a costumer, where they noted a power generation of 430W, even if no power generating equipment was installed in the household. The installed meter used a Rogowski coil for current sensing. This peculiar situation was analyzed and reproduced in a controlled lab environment. The tested load was a TV and a remote with dimming functionality (even if the costumer reported that only switch functionality was intended). The situation was reproduced with an ideal power supply and the power grid of the building. In both cases the onsite observations were confirmed. The wave-forms causing the erroneous power generation were investigated, and it was observed that the dimming function of the remote phase-shifted the current pulse, with a variable FA of 45, 90 or 135 degrees. It was noted that no error was measured with a FA of 90 degrees, while the FA of 45 and 135 degrees resulted in opposite sign deviations, with a negative power consumption of -452W for 45 degrees and positive deviations of 661W for 135. Additionally, it was noted that the error adds up when multiple remotes are connected. Finally, the effect of the pulsed current signals using a Rogowski coil, Hall sensor and CT is studied in [4]. In that paper, a dimmed water pump with firing angles of 45 and 135 degrees is used as a load together with 4 restive loads (heater). It is shown that no error occurs for the linear resistive loads, while errors of 30% and 35% are measured for the non-linear loads. A root cause analysis is performed, which identified a saw-tooth wave as output of the current sensors when no current was flowing, for both Rogowski coil and CT. The saw-tooth response behaviour can be seen in Fig. 1. On the other hand, research is missing regarding the origin of the saw-tooth response for static meters using CT metering. In this paper, a meter known for resulting in metering error is analyzed. This meter uses CT for current metering. Firstly its metering circuits are identified, allowing to measure internal signals; a linear resistive load is then used to tune the equations modelling the power calculations from such signals. Finally

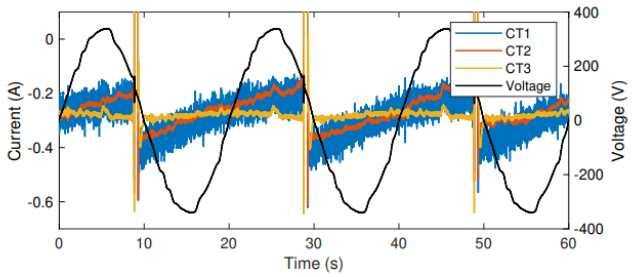

Fig. 1: Measured current for Rogowski coil (blue), Hall sensor (yellow) and current transformer (orange) [4]

the same pump used in [4] is tested, in order to identify the properties and characteristics of the metering errors. A root cause analysis is also performed, by testing the CT with a laboratory power supply and different wave forms, as well as simulations using LTSpice.

This paper will be organized as follows: Section II presents the testing setup and equipment used for testing; Section III presents a reverse engineering of the internal circuitry of the smart meter, including a block diagram and power equations from the sensed signals; Section IV identifies the sources of metering errors for non-linear loads; a root-cause analysis is performed in Section V, while Section VI analyzes the implications of the undesirable behaviours on the metering; finally Section VII summarizes and concludes the paper.

II. Method

In order to test the smart meter readings, a simple setup is used, connecting the smart meter to the laboratory grid and a load. Additionally, a voltage probe Pico Technology Oscilloscope Probe TA043 and current clamp Pico Technology TA189, known for providing accurate measurements also for non-linear loads, are used to compare the SM readings and retrieve the error. The reference voltage and currents are referred as V_{ref} and I_{ref}. A schematic for the 1-phase testing setup is shown in Fig. 2.

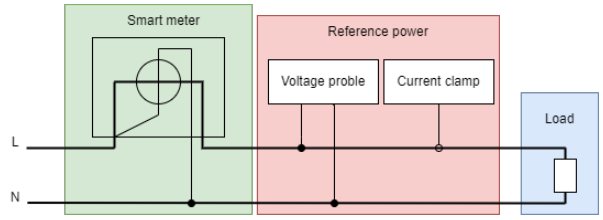

Fig. 2: Setup schematic for 1-phase measurements, displaying the meter, the probes for reference power and the load

The loads used during testing are:

- TE2000B10RJ power resistor 100Ω
- resistive heater with selectable power draws, ranging from 190 to 1800W
- water pump with dimming functionality

The heater and power resistors are used for testing the setup on linear loads, resulting in sinusoidal current draws, while the water pump is a non-linear load. It draws a pulse current, with high amplitude, high d*i*/d*t* and crest factor. The remote allows to set ten dimming levels, corresponding to different amplitude and FA of the pulse. The pulse parameters are detailed in Table I, and each current draw waveform can be seen in Fig. 3. Note that while each pulse presents different amplitude and waveform, throughout this paper an ideal square wave with low duty cycles is used for simulation purposes. The primary current and voltage of the CT are referred as reference signals, since they are used in error calculations.

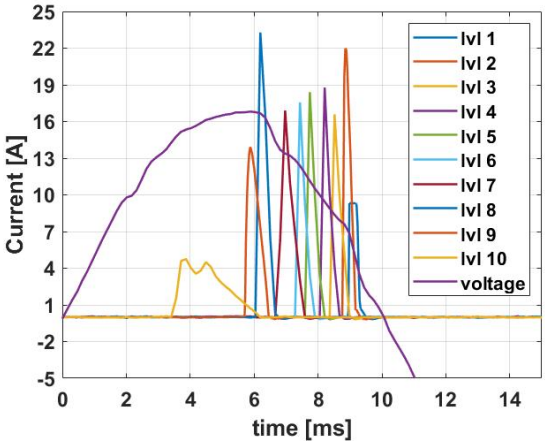

Fig. 3: Current draw for pump level

TABLE I: Water pump level and corresponding pulse parameters

Pump Level	FA [deg]	Amplitude [A]	Pulse width [ms]	Power [W]
1	162	9.3	1.0	15.4
2	154.8	21.8	5.1	34.7
3	150.4	16.6	6.2	36.7
4	142.2	19	7.7	44.6
5	136.6	18.4	6.2	51.5
6	127.8	17.5	0.7	54.7
7	122.3	16.8	0.9	85.9
8	108.7	23.2	0.8	106.9
9	100.8	13.6	0.8	100.8
10	81	4.9	2.6	115.2

III. Inside the smart meter

The smart meter in question presents two sensing circuitry, a CT for current sensing and a resistive divider for voltage sensing. By following the PCB traces and using continuity tests, the overall circuitry was retrieved and a schematic was made, which is analyzed in more detailed in Appendix A. In this section, only the relevant circuitry for current and voltage sensing is analyzed. Simplifications and equivalent circuit principles are applied for ease of understanding and readability. Overall, the operation of the circuitry can be modelled using a block diagram, shown in Fig. 4. It can be seen that the resistive divider is used to measure the supply voltage, while current is instead measured using a CT, followed by a transimpedance amplifier (TIA) used for converting the secondary current into a voltage signal to be measured by the microcontroller unit (MCU). Each of those

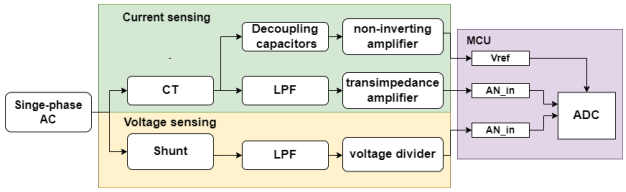

Fig. 4: Block diagram of sensing circuit, including current metering using a CT, and voltage metering using a voltage divider

parts is analyzed in more detail in the following subsections, while the amplifier is detailed in Appendix A.

A. Current Sensing

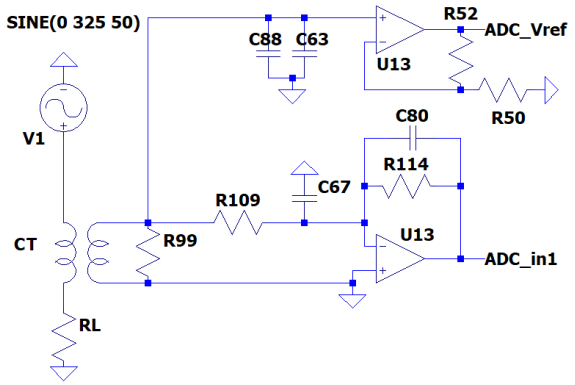

Fig. 5: CT circuit, including low pass filter, TIA and active amplifier

The relevant circuit for the CT is shown in Fig. 5. The CT's primary coil is connected in series to the load. The varying magnetic field in the primary coil induces a current on the secondary coil, equal to the primary current multiplied by the ratio of turns. The secondary current is then input of a TIA, converting it into a voltage signal to be measured by the MCU. Using a linear, resistive load, the input and output of the amplifier block can be compared to understand its behaviour. It was measured that it amplifies the signal with a factor of 32.25, determined by the ratio of resistors R3 and R2, as well as low pass filter for high frequency noise, with a cut-off frequency of about 60KHz. The output signal of the TIA block is what is used for power calculation, and in this paper is referred as 'measured current signal'.

B. Voltage Sensing

Voltage is sensed through a voltage divider which scales the signal to the MCU's ADC range. Throughout this paper the output of the voltage divider will be referred to as 'measured voltage'.

C. Power calculation

From the sensors described before, power can be calculated. It is worth noting that the signals measured using the oscilloscope probes are scaled to the ADC range (0-5.2V) and have a DC offset of 2.5V. In order to reconstruct the original waveform, the DC offset is first removed from the measured signal, and this is then scaled with a factor G to the correct amplitude.

$$i_p = G_{ct} * (V_{ct} - 2.5) \tag{1}$$

$$V = G_{sh} * (V_{sh} - 2.5) \tag{2}$$

Finally, the instantaneous power is calculated by multiplying the current and voltage signals. Average power is then calculated as:

$$P_{average} = \sum_{n=1}^{N} \frac{P_i}{N} \tag{3}$$

Using the linear 100Ω resistor as load, the measured signals can be compared to the reference ones, and the gain factors are calculated:

- $G_{ct} = 1.6775$
- $G_{sh} = 183.42$

IV. Metering Errors

The water pump is connected as a load as shown in Fig. 2. By comparing the reference and measured signals it is possible to identify the origins of the power metering deviations. Fig. 6 displays the reference and measured signals for the pump at level one. It can be noted that while the voltage is accurately measured, two issues are present on the current metering instead: clipping of the pulses at about 4.5A, and the droop along the areas of zero current in between pulses. When the primary pulses drops to zero, the measured one does not follow it accurately, but instead drops to a value below zero, and then slowly settles. Because the next pulse starts before the value settled, each pulses has a starting value different than zero as well. A close up of the droop and slow settle is shown in Fig. 7.

V. Root Cause Analysis

In this section a root cause analysis is performed to identify the cause of the undesirable behaviour in the current measurement.

A. Droop

In order to analyze the current response for any arbitrary wave-form, the CT is removed from the meter and used in a test set up as shown in Fig. 8. R_p is used to limit the current through the primary coil, R_s is the resistance of the secondary coil while R_L is the burden resistor. The power supply used is an HP3314A function generator. Note that a burden resistor is used to convert the current into a voltage signal. A large value is chosen (about 1kΩ) also to allow for a shorter time constant, for ease of measurement and presentably of results. Ideally, in a CT, the secondary current is a perfect replica of the primary one scaled by the the turn ratio. Yet, in order to maintain a secondary current, a change in flux, and therefore primary current, is needed. However, a square wave has large DC components at the top and in between pulses. In an ideal transformer, the secondary current and voltage will instantly drop to zero, as is shown

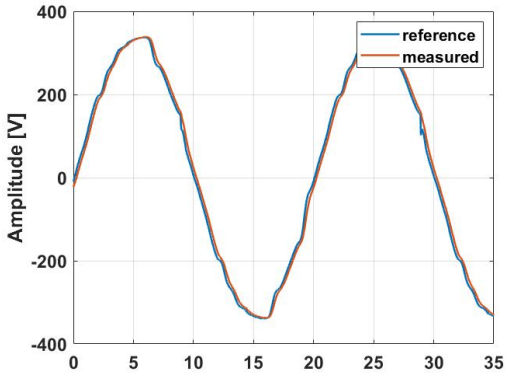

(a) Measured and Reference voltage signal

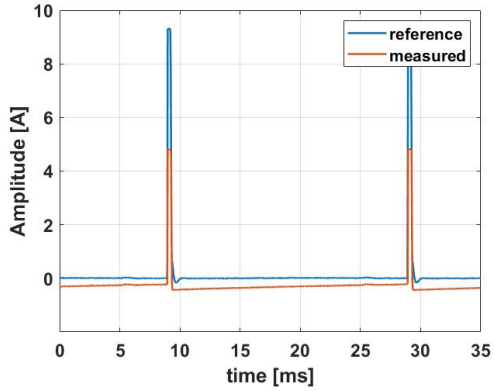

(b) Measured and Reference current signal

Fig. 6: Measured and reference signals for pump at dimming level 1, where clipping and droop occurs for the current metering

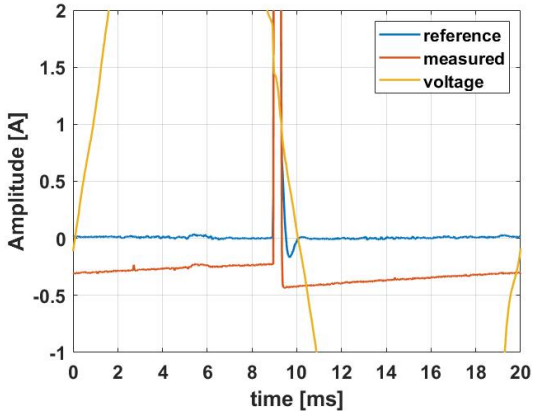

Fig. 7: Close up of the drift issue

in Fig. 9, performed using a simulated ideal transformer. On the other hand, in a non-ideal transformer, the core presents a magnetization behavior. As proposed in [5], an equivalent circuit can be used to accurately model this phenomena, by expressing the secondary coil as a current source and a variable inductor L_e modelling the magnetizing behaviour of the core. The equivalent circuit, shown in Fig. 10, will then present an RL exponential response. It is worth nothing that, when approaching saturation, the impedance of L_e will decrease,

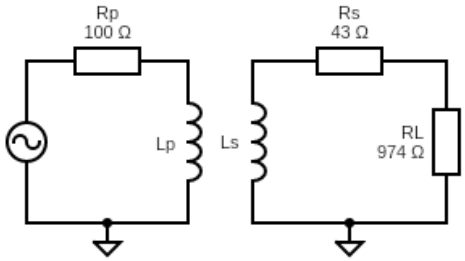

Fig. 8: Test setup for CT, where Rs is the internal resistance of the secondary coil, R_L is the load and R_p is a current limiting resistor on the primary coil

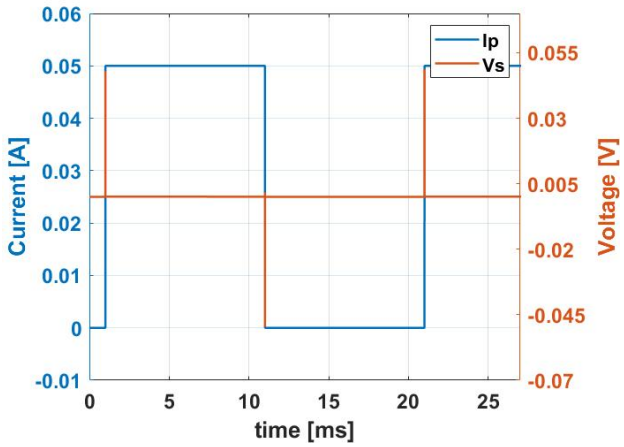

Fig. 9: Simulated primary current and secondary voltage in ideal CT, with voltage corresponding to the derivative of the primary current

since the core is unable to provide the change in flux, resulting in a reduction of current across the load. However, during testing saturation was not identified in operating conditions: with a pulse peak of 25A, no change in inductance was measured (see Fig. 13 at 25A compared to Fig.12 at 0.02A). The magnetization inductor will therefore be treated as a normal inductor with fixed value. See Appendix B for more details about core saturation. In the equivalent circuit, the current source represents the ideal secondary current, equal to the primary current scaled by the CT ratio. In areas of no change in primary current, the voltage across the load will drop as described by an exponential function, dependent on the time constant $\tau = L_e/(R_s + R_L)$. The value of the inductor can then be calculated by comparing the discharge time of the inductor with the time constant equation. By applying a pulse signal, the discharge time is measured to be approximately $8.3ms = 5\tau$, from which the inductor value can be calculated as 1.69H. This discharge behavior can be seen in Fig. 11 for a square wave primary current with a duty cycle of 50%. However, when the square wave width becomes shorter then 5τ, the coil does not have time to discharge before the negative pulse starts. This results in an asymmetrical behaviour where the positive peak is larger than the negative peak, resembling

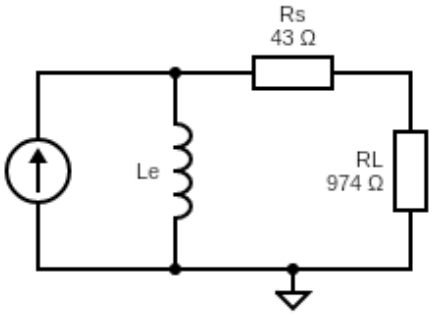

Fig. 10: Equivalent CT circuit

the behaviour seen for the pump response. A 50Hz pulse with a peak amplitude of 10V and a duty cycle of 5%, corresponding to a width of 1ms, less than the time constant of the circuit, is applied to the CT. Such square is used to emulate the current draw of the water pump. The mentioned behaviour can then be seen for both simulations and measurements on the actual CT, as seen in Fig. 12.

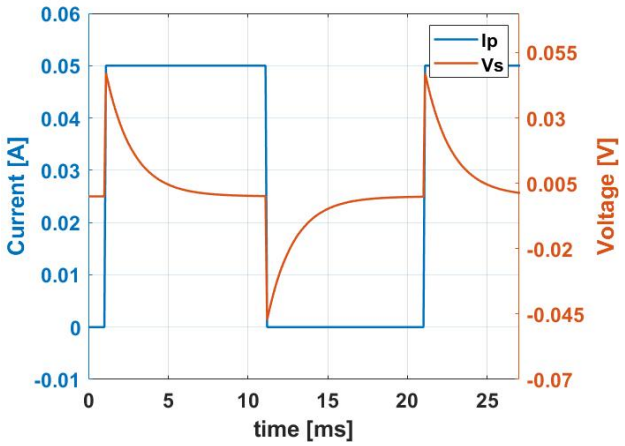

Fig. 11: Simulated primary current vs output voltage for non-ideal CT and primary pulse $\geq 5\tau$

Through the analysis above, it was possible to accurately simulate and verify the response of a CT to square wave primary currents, including the effects of the magnetization of the core. It is then possible to simulate the sensing circuit of the meter in question: the burden resistor is set to 35.7Ω, and then connected to the TIA as for circuit schematic (see Fig. 5). Note that the low-pass filtering capacitor is ignored since the noise filtering aspect is not relevant for this paper. The simulated schematic is shown in Fig.14. With a burden resistor of 35.7Ω and the low impedance of the TIA, the time constant will increase to approximately 20ms, since the equivalent resistance is reduced. Because of the large value of the new time constant, any 50Hz pulse will result in a pulse width shorter than the RL discharge time, incurring in the asymmetric behavior shown in Fig.12. Additionally, the effect of the large time constant is also seen in the slow settling time

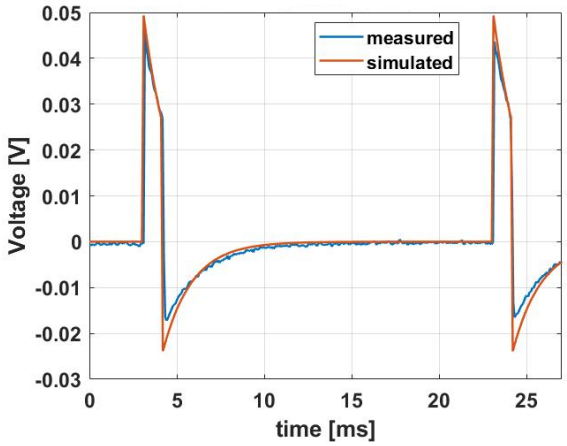

Fig. 12: Simulated and measured secondary voltage, showing asymmetrical behavior when pulse width is shorter than the RL discharge time

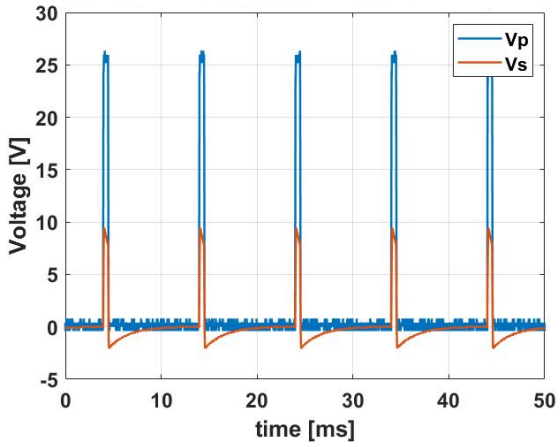

Fig. 13: RL discharge behaviour for 25A primary current, resulting in 1.66ms time constant, identical for the 0.2A behavior

to zero. In case of a 50Hz pulse shown in Fig. 6, the next pulse starts before the output voltage has settled to zero, causing the pulse to start at a negative value. A simulation of the circuit is performed, resulting in an output voltage as shown in Fig. 15. The response resembles the problematic waveform detected on the actual meter for the pump. A case of a larger period between pulses is shown using simulations in Fig.16 instead, showing the complete discharge curve.

B. Clipping

In Fig. 6, it was noted that the current measurement clips at the output of the TIA. When the primary current amplitude is larger than 4.5A, the resulting voltage of the TIA has a voltage swing larger than the operating range of the op-amp, causing the signal to clip at the ground and positive rails. This clipping is then propagated backwards through the feedback path, clipping the secondary voltage of the CT as well. The clipping at the TIA and CT secondary voltages can be seen in Fig. 17.

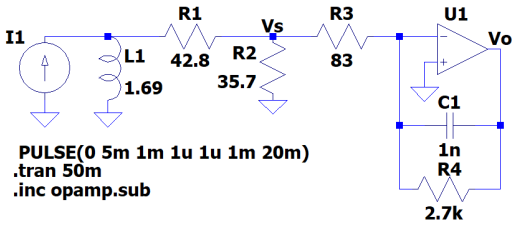

Fig. 14: Circuit including TIA stage, used to convert the current into a voltage signal

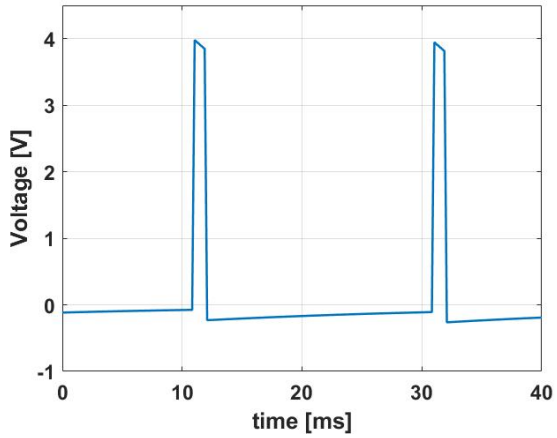

Fig. 15: Simulated output of circuit with large settling time, when a 50Hz pulse is applied

VI. Implication on Metering

In this section, the implication of the issues identified before on the power metering are analyzed.

A. Clipping

Firstly, the clipping issue is covered. As can be seen in Fig. 6, the current signal clips at an amplitude of about 4A. Upon further investigation, it was noted that by reversing the polarity of the load, the current signal clips at a different magnitude (4.2A and 4.5A). This difference is caused by the DC component of 2.5V, which cause asymmetric clipping at the op-amp range of 0 to 5.2V. While resistive loads are symmetric and the error won't be affected by load polarity, when using loads such as the water pump that draw asymmetric pulses, the magnitude of the error will differ depending on the orientation. Also, because the meter is to be used for households appliance, it can be surprising to find that the current signal clips at 4A already, where loads that draw up to 10A are not unusual. This was also confirmed by loading the system with the heater: with a resistance of 66Ω (800W), a peak current of 5.2A was expected, but the measured signal is clipped at -4.2 and 4.5A, as shown in Fig. 19, comparing resulting current measurements vs reference signal on a linear load. The sampled power calculated using the measured current and voltage corresponds to an error of about -7%. On the other hand, the meter reading resulted in an error of less than -2%. For this reason it is believed that the internal software of the meter detects and corrects for the

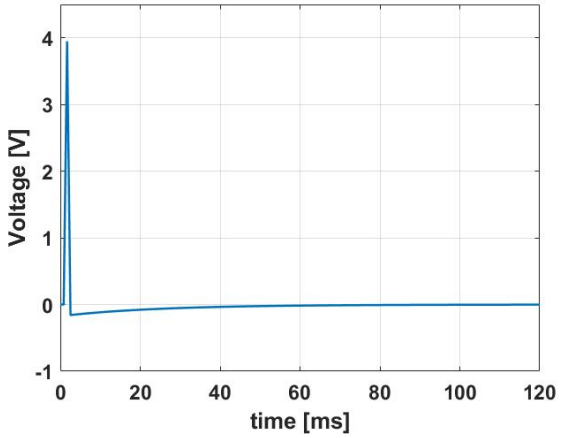

Fig. 16: Simulated output with large period between pulses, showing slow RL discharge times

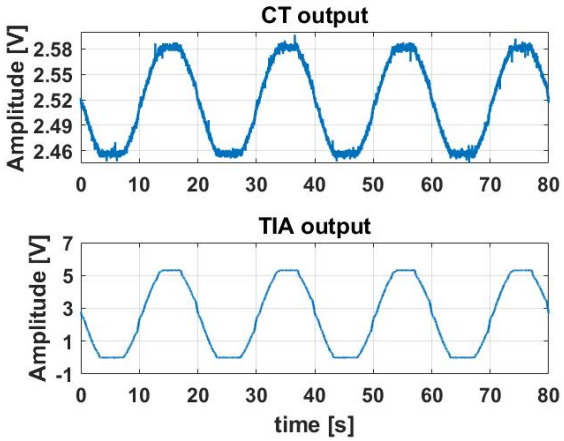

Fig. 17: Clipping of signals for linear resistive load (66 Ω), resulting in CT secondary voltage clipping

clipping of a sinewave. Moreover, because the different pump levels have different pulse amplitudes, the contribution of the clipping to the total error varies with the pump level. In order to only estimate the contribution of the clipping to the error, the measured signal is reproduced from the reference one by clipping it at amplitudes of -4.2 and 4.5A, and then measuring the power deviation between the original and clipped one. All measurements are done for a single period. The result is listed in Table II. The amount of error caused by clipping is determined by the amplitude of the current pulse, since current draws larger than about 4A will cause the signal to clip.

B. Droop

The other issue noted above was the non-zero value of the secondary CT current in between primary current pulses. It can be seen that even as the primary current settles back to zero, the current measured by the meter drops to a negative level instead, and slowly drifts back towards zero. The contribution of the drift in the total metering error depends on the FA of the pulse: the position of the pulse relative to the sinusoidal voltage determines if the current drift contributes to a positive

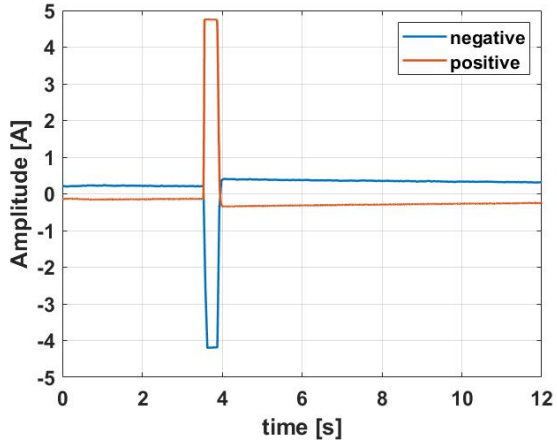

Fig. 18: Clipping with opposite load orientation, resulting in different clipping values

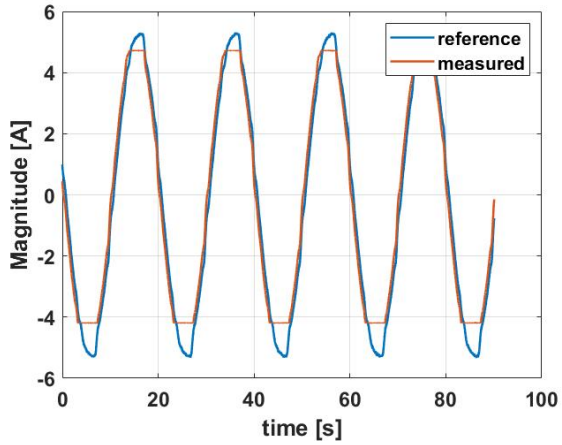

Fig. 19: Measured and reference current for linear loads, notice the clipping at asymmetrical values

or negative estimation. An example of positive or negatives contribution is detailed in Fig. 20 for pump level 1, where areas of positive or negative contribution are marked. The total error is determined as the sum of positive and negative contributions. It then becomes clear that the FA will affect the magnitude and sign of the power estimation.

In order to simulate the effect of the FA on the clipping on the error, a one period measured pulse is taken for pump level 1. The reference is then also clipped at the same magnitude, isolating the error due to the drift. The signal is circle-shifted over one period, corresponding to firing angles between zero and 180 degrees, and for each FA the difference between measured and reference power is calculated. Finally, the resulting power error is plotted against the phase in Fig. 21. It is worth considering that the resulting simulation is rendered inaccurate by the assumption taken:

- current waveform supposed identical for each pump level. This is not the case, as was shown in Fig. 3.
- no parasitic effects of setup, wires and probes
- no external EMI

Nevertheless, the simulation is useful for identifying the over-

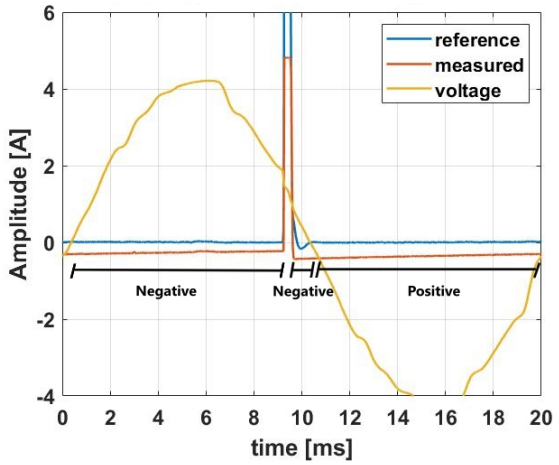

Fig. 20: Positive and negative error contribution for a specific FA. Different FA result in different areas of positive or negative error

all correlation between FA and resulting metering error. This shows the possibility of both negative or positive deviations, with a firing angle of 90 degrees resulting in minimal absolute error. Finally, the droop error is calculated for each pump level,

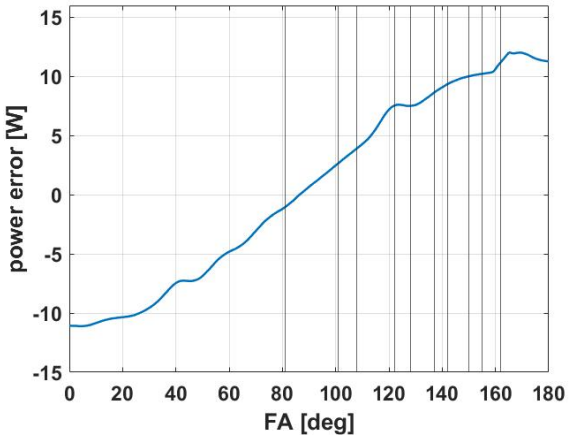

Fig. 21: Simulation of error for FA of the pulse, resulting in positive or negative error contributions

again ignoring the contribution of the clipping by also clipping the reference signals. A comparison between simulated and measured drift error is shown in Fig. 22, with vertical lines marking the pump levels in descending order. Numerical data is listed in Table II. An additional remark to note is the correlation between the pulse width and the droop error. In particular, the shorter the pulse width, the smaller the droop effect and therefore less negative secondary current flow. This is due to the fact that there is less discharge at the top of the pulse, resulting in smaller negative peaks.

C. Total error

Table II summarizes the data collected in the previous subsections, including the contribution of the clipping, of the drift and the total error. Through the above analysis, it was possible to identify the major issues in current sensing, as well as

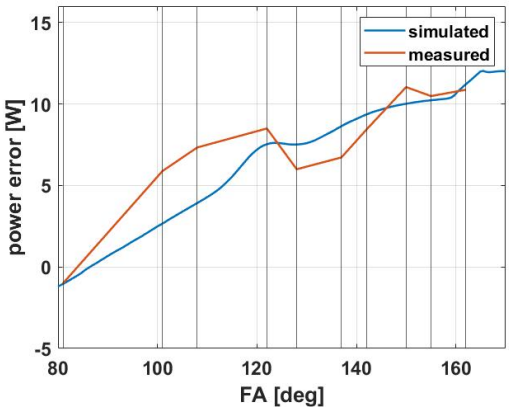

Fig. 22: Comparison between simulated and measured errors due to droop, matching in overall trend. Vertical lines correspond to pump levels in decreasing order.

determining its implications in metering errors on the current setups. In particular it was noted that, when a primary pulsed current is applied on the CT, the magnetization of the core, modelled as a parallel inductance, causes the secondary current to not accurately match the primary's current waveform. The response presents instead an exponential discharge in areas of no change in current, such as the top or in between pulses, resulting in secondary current droop. Note that an ideal square wave is used for those considerations in order to represent the pulsed current draw of the water pump tested. Additionally, when the pulse is shorter than 5τ, the secondary CT voltage will present the asymmetric behavior detailed above, and, together with the large time constant, causes the asymmetric current response measured during testing. While this response resembles a pulse, it does not accurately represent the primary current. When simulating the effect of the FA on the error, it was noted that minimal error is present for angles of 90 degrees, with maximum positive error for angles around 180 degrees and negative around zero degrees. When comparing the simulated plot with the pump measurements, it can be taken remark that, while the overall trend is followed, some deviations are present, particularly for pump levels 2 to 6. This deviations are mostly the result of the assumptions taken for simulating, such as the fact that all current draws are supposed identical for pump level 1 to 10. In reality, each pump level presents different amplitude and pulse shape, as shown in Fig. 3. Nevertheless, those finds confirm the correlation between FA and deviations found in [2]. Additionally, the limited range of the transimpedance amplifier op-amp causes the signal to clip. This occurs for currents above 4.5A, but little error was detected by the meter using linear loads, even with currents above clipping level. This seems to suggest software compensation, but this is outside the scope of this research. The clipping issue can also be specific to the meter model, therefore more research is required into this topic. Finally, this analysis allows to demonstrate that CT sensing results in large current metering errors. This empathizes the need for additional testing of installed meters to identify those effects, preventing over-billing of the costumers by the hands of utility companies. For more details about the societal impact of these finding, see Appendix C.

TABLE II: error contribution for pump levels

Pump Level	FA [deg]	Clipping error [W]	Droop error [W]	Total error [W]
1	162	-6.6	10.2	3.6
2	154.8	-22.5	10.5	-12.1
3	150.4	-19.8	11.0	-8.7
4	142.2	-26.1	8.4	-17.6
5	136.6	-30.7	6.7	-24.0
6	127.8	-31.0	6.0	-25.0
7	122.3	-42.8	8.5	-34.3
8	108.7	-74.0	7.3	-66.6
9	100.8	-49.0	5.9	-43.0
10	81	0	-1.0	-1.0

VII. Conclusion

In this paper an analysis on power metering interference caused by pulsed currents was performed on static meters using current transformers. In particular, the limitations in metering non-linear loads that draw pulsed currents are identified, concluding that CT with large magnetization inductance are not appropriate for pulsed current metering. This is due to the magnetization behavior of the core, modelled as a parallel inductance, resulting in CT secondary RL discharge, paired with the large DC components of pulsed wave-forms. Additionally, when the pulse width is shorter than the RL discharge time, the secondary current will present an asymmetric behavior, as seen during measurements. It is worth noting that this asymmetric behavior allows to reconstruct a pulse similar to the primary current, with an error due to the negative peak and slow settle towards 0. This error is smaller for small pulse widths, since the negative peak is reduced. Measurements and simulations also confirm previous research correlating the value of the FA with the deviation magnitude and sign, with the possibility of both positive and negative deviations. On the other hand, more research is needed to accurately identify the relation between pulse width and metering error for pulses causing asymmetrical response. A second identified issue is the clipping of the TIA output, but this issue might be limited to the tested meter. In conclusion, it can be stated that, when CTs are used for pulsed current metering, its operating range is not only limited by its frequency range, but also by the magnetization behavior of the core and the pulse width. This indicates a need of additional testing, even for meters compliant to [1], covering the effects of pulsed currents with small duty cycle, high di/dt and crest factors. Proper testing will therefore ensure fair power metering, and prevent both over and under-billing of costumers by the utility companies.

References

[1] IEC61000-4-19, "Electromagnetic compatibility (emc)-part 4-19: Testing and measurement techniques - test for immunity to conducted, differential mode disturbances and signalling in the frequency range from 2 khz to 150 khz, at a.c. power port," in 2014.

[2] F. Leferink, C. Keyer, and A. Melentjev, "Static energy meter errors caused by conducted electromagnetic interference," *IEEE Electromagnetic Compatibility Magazine*, vol. Volume 5, 2016.
[3] B. ten Have, N. Moonen, and F. Leferink, "How to earn money with an emi problem: Static energy meters running backwards," *2021 IEEE International Joint EMC/SI/PI and EMC Europe Symposium.*, 2021.
[4] ——, "Electromagnetically interfered energy metering resulting from droop of current transducers," *2021 IEEE International Joint EMC/SI/PI and EMC Europe Symposium.*, 2021.
[5] A. Hargrave, M. J. Thompson, and B. Heilman, "Beyond the knee point: A practical guide to ct saturation," *71st Annual Conference for Protective Relay Engineers*, 2018.
[6] RENESAS, *M16C/6C Group Datasheet*. 2012.

Appendix A
Circuit schematics

The simplified sensing circuit is shown in Fig. 23.

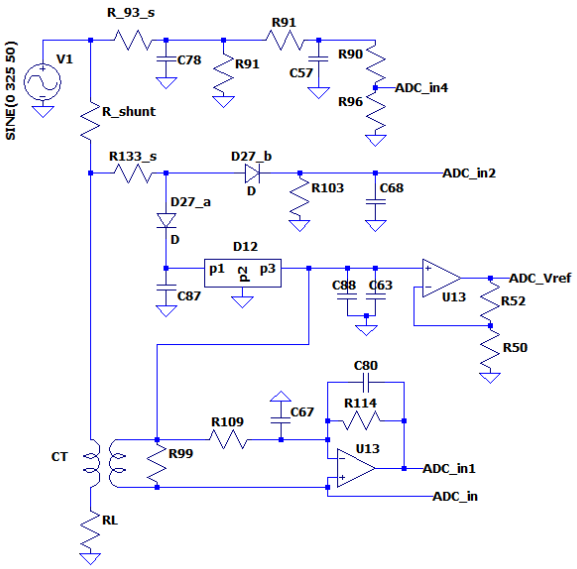

Fig. 23: schematic of sensing circuit

The two sensing circuits can be identified with the shunt resistor at the top, and the CT at the bottom connected to the two operational amplifiers. RC couples are used for low pass filtering (such as R91 C57 or R109 C67), as well as decoupling capacitors, such as C88 and C63. Finally, the CT secondary voltage is also passed through a non-inverting amplifier. Its output is a 5V signal used as voltage reference in the ADC and DAC of the microcontroller, used to set the voltage range it operates at [6]. This voltage level is generated by setting a high gain factor R52/R50, clipping the output to the op-amp rail.

Appendix B
Saturation

In an ideal CT with a 1:1 turn ratio, the secondary current I_s is a perfect replica of the primary current I_p. However, in a real transformer, saturation can occur, resulting in a secondary current which does not replicate the primary current. The reason a CT saturates is due to the physical properties of the iron core: the core can be visualized as a fixed number of molecular dipoles, whose polarity is randomly arranged. The varying current in the primary coil generates a magnetic field H, which causes the dipoles in the core to align in the same direction as H. The number of align dipoles at a moment in time is called flux density (B): the change in flux caused by the arranging of the dipoles induces current on the secondary coil. [5] Different materials have different B-H curve, an example is shown in Fig. 24. In vacuum, once all the dipoles are aligned,

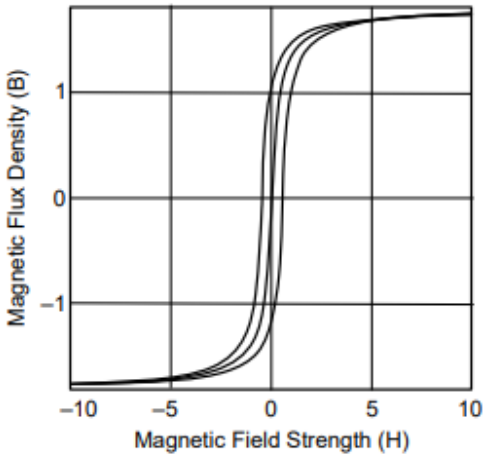

Fig. 24: Example of B-H curve [5], expressing non-linearity of B-H relationship

no more change in flux can be provided by the core, and the secondary current drops to zero. In a real setup, even as the CT saturate, some leftover change in flux can still be provided by the surrounding material and air. Similarly, approaching the area of non-linearity of the B-H curve close to saturation will cause a decrease in amount of change in flux produced, which is still sufficient to maintain a secondary current, but not enough to follow the primary current, resulting in output clipping. On the other hand, saturation does not occur in the testing conditions in this paper, as was shown before by applying a high amplitude primary current in Fig.13 (25A) and 25 (10A) .

Appendix C
Societal impact

As mentioned before, the combination of CT sensing and pulsed primary currents resulted in high power metering deviations. Customers reported a sudden increase in power bills after replacing the old electro-mechanical meters with the newer smart meters, but after reporting to the utility companies, their complaints were rejecting, stating that mechanical wear on the old meter caused them to be under-billed for years [2]. At most, companies would send a technician to test the faulty meter at the expense of the customer, but because the test standards only focused on linear loads, no issue was detected. However, this paper presents evidence in

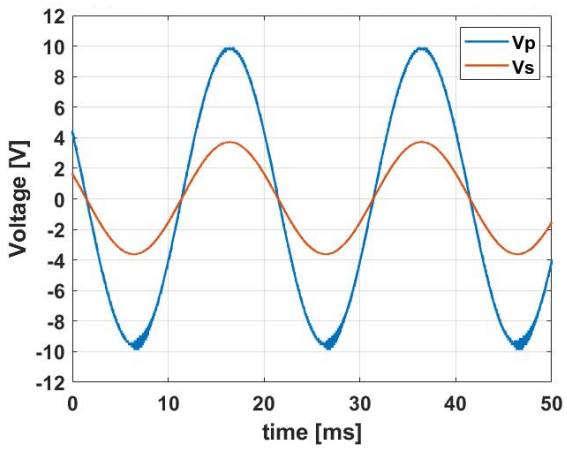

Fig. 25: Primary and secondary voltage for restive load on CT. Note that no clipping occurs at the secondary output, even with a primary current of 10A.

support of the case that pulsed currents result in erroneous power metering, and confirming that the customers are indeed being over-billed. Particularly, the need for additional testing, covering the effects of non-linear loads that draw pulsed currents is emphasized. This will allow to support the customer case against the utilities for fairer metering and therefore billing. In the opposite case, such testing would prevent or discourage events such as in [3], where power companies can be protected from losses in case of intentional or accidental negative metering deviations.